A DYNAMIC, COUPLED THERMAL RESERVOIR APPROACH TO ATMOSPHERIC ENERGY TRANSFER PART II: APPLICATIONS

Roy Clark, Ph.D.

Ventura Photonics

1336 N. Moorpark Road #224

Thousand Oaks, CA 91360 USA

ABSTRACT

The coupled thermal reservoir approach described in Part I is demonstrated by analyzing flux and meteorological data covering a range of thermal reservoir conditions. These include mid latitude ocean thermal storage, the surface flux balance of the Pacific warm pool and the land surface flux balance in S. California. In addition to temperature data, the effects of thermal gradients, flux interaction lengths and the time delay or phase shift between the heating flux and the temperature response are considered. Long term climate trends in weather station minimum meteorological surface air temperature (MSAT) data are also analyzed. For selected California and UK weather stations these follow the regional trends in ocean surface temperature. This allows urban heat island effects and other weather station biases to be investigated. The effect of a 100 ppm increase in atmospheric CO_2 concentration on these data sets is shown to be too small to be measured.

Keywords: Carbon Dioxide, Dynamic Coupled Thermal Reservoirs, Greenhouse Effect, Interaction Length, Meteorological Surface Air Temperature, Ocean Warming, Phase Shift, Radiative Transfer, Thermal Storage, Urban Heat Island Effect.

1. INTRODUCTION

The basic concept of coupled thermal reservoirs was presented in Part I in the previous paper. The surface temperature is determined by the time dependent flux balance of a series of coupled reservoirs. In addition to the temperature, there are three other important parameters need to be considered. The first is the thermal gradient, the second is the interaction length (depth or path length) and the third is the time delay or phase shift between the incident flux and reservoir thermal response. Here in Part II, the application of this concept to specific reservoir properties is demonstrated using examples based on measured flux and meteorological data.

First, the thermal storage properties and the effects of wind driven evaporation on the flux balance of the ocean reservoir is considered using data from the Argo Float Program and the Triton Buoy network.[1,2] The phase shift or seasonal delay between the solar flux and the ocean

thermal response at mid latitudes produces significant thermal storage effects. Maximum ocean surface temperatures in the Pacific warm pool are determined by the flux balance between the solar heating and the wind driven surface evaporation. The wind speed also influences the diurnal surface temperature rise and the related phase shift. Then the flux balance of the air-land thermal reservoir interface is addressed by considering the flux data from a measurement site located near Irvine in S. California.[3] In addition, the thermal storage properties of the lower tropospheric reservoir are investigated using radiosonde data from the Miramar, San Diego monitoring station.[4]   Finally, the influence of ocean surface temperatures on the measured climate trends from meteorological stations in California and the UK is considered. The changes in ocean surface temperatures resulting from the Pacific Decadal Oscillation (PDO) or the Atlantic Multi-decadal Oscillation (AMO) provide climate reference baselines that may be used to identify urban heat island effects and other station bias effects.[5,6] The effect of a 100 ppm increase in atmospheric CO_2 concentration on the recorded data is also considered and the effects are shown to be too small to measure. The increase of 1.5 W m^{-2} in the downward LWIR flux from CO_2 is coupled to the total net surface flux. The large heat capacities and the large flux and flux variation terms simply overwhelm the effects of a small increase in LWIR flux from CO_2. This follows from the dynamic surface flux balance discussed in relation to Eqns 1 through 8 in Part I.

2. THERMAL STORAGE IN THE OCEAN RESERVOIR

At mid latitudes, the ocean is heated by the sun during the summer and cools by excess wind driven evaporation in winter. A stable subsurface thermal gradient forms as the sun heats the ocean and this is removed in winter as the additional cooling increases the depth of diurnal mixing layer.[5,7] There is also a time delay or phase shift between the maxima and minima in the solar flux and the ocean temperatures. The seasonal heat storage is substantial and plays a major role in stabilizing the mid latitude climate. At 45° latitude, the peak cumulative 'clear sky' daily solar flux is approximately 25 MJ m^{-2} day^{-1}. The winter solar flux decreases to 5 MJ m^{-2} day^{-1}.

Figure 1 shows the ocean temperature profiles for 2007 recorded by an Argo float drifting near 42° S, 153.5° W in the mid S. Pacific Ocean.[1,7] The peak summer/fall temperatures are between 288 and 289 K (15 and 16 C) at 5 and 25 m depth. During the winter/spring, the ocean cools to 283 K (10 C) down to depths of 100 m. (Seasons are reversed in the S. Hemisphere). Peak ocean temperatures are reached in late February, 2 months after the solar flux peak. Ocean cooling continues until the end of October, some 3 months after the solar flux minimum. These time delays or phase shifts are characteristic of large scale thermal reservoirs. Figure 2 shows the change in heat content (deviation from the average) calculated from the temperature data in Figure 1. The heat content fluctuates because the float is drifting. However, the total annual change in the heat content is approximately 1000 MJ m^{-2}. Most of this is stored in the first 75m

ocean depth. This heat storage corresponds to ~40 days of full summer sun. The accumulation of heat during the summer and subsequent release in winter stabilizes the Earth's mid latitude climate. The short term peak to peak fluctuations in ocean heat content are approximately 100 MJ m^{-2}. The total annual increase in downward atmospheric LWIR flux for a 100 ppm increase in atmospheric CO_2 concentration is only 50 MJ m^{-2} and none of this can penetrate more than 100 micron into the ocean surface. This is approximately the same interaction length as the surface evaporative cooling. The magnitude and variation in the solar and surface evaporative cooling flux are too large for a 100 ppm increase in CO_2 concentration to have any measurable effect on the reservoir temperatures.
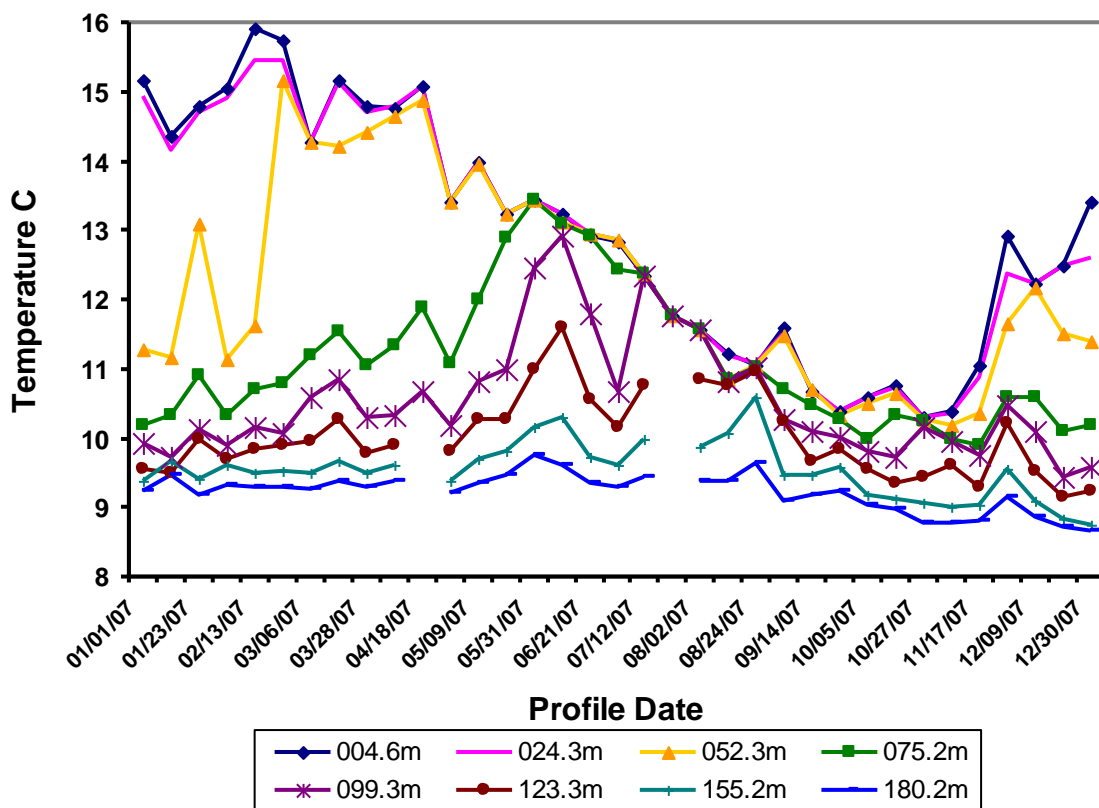

Figure 1: 2007 Argo float ocean temperature profiles near 42° S, 153.5° W in the mid S. Pacific ocean.
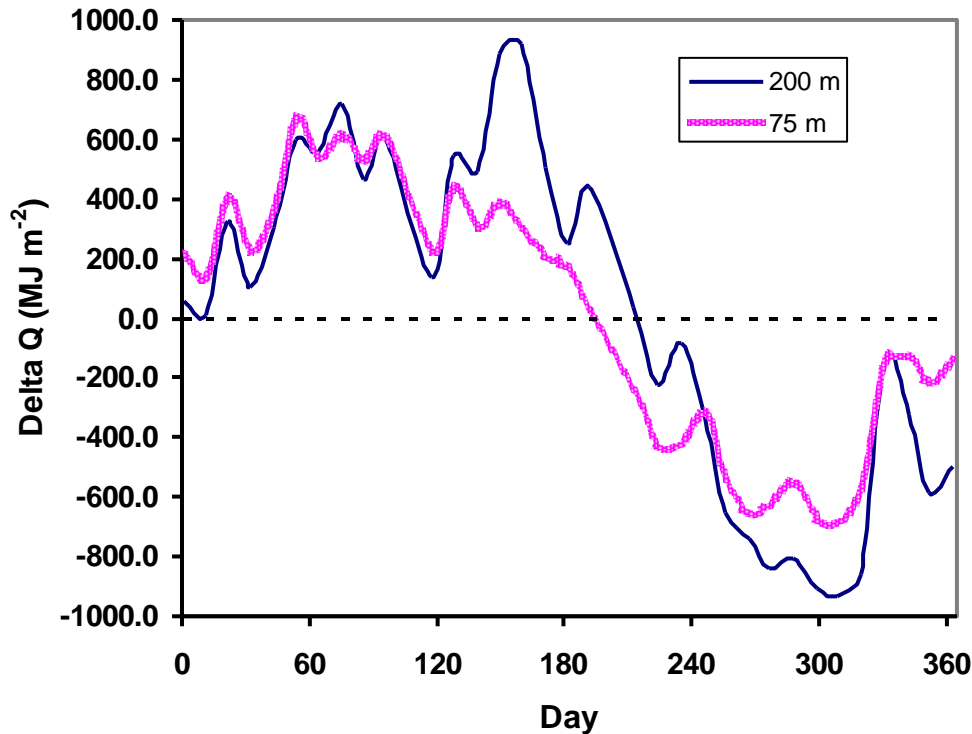
Figure 2: Change in ocean heat content calculated from the data in Figure 1, MJ m^{-2} for 75 and 200 m depth columns.

3. SURFACE ENERGY TRANSFER IN THE PACIFIC WARM POOL

Half of the total solar flux incident on the Earth's surface falls within the ±30° latitude bands. The coupling of the convective flux rising in the tropics to the Earth's rotation establishes the Hadley cell circulation, the trade winds and the large scale ocean gyre circulation. The N. and S. Pacific equatorial currents are the east to west circulation components of the N. and S. Pacific gyres. They are fed by cool ocean water flowing from higher latitudes along the west coast of the Americas (Humboldt and California currents). As the ocean water flows across the equatorial Pacific Ocean it is heated by the tropical sun. The full 'clear sky' solar flux varies between approximately 22 and 25 MJ m^{-2}.day^{-1} and the peak flux occurs at the equinox points. The evaporative cooling in the eastern equatorial Pacific is insufficient to balance all of the absorbed solar flux and the ocean temperatures increase as the water moves westwards. Here it accumulates in the western Pacific warm pool. The ocean surface temperature is near 303 K (30 C) and the pool may extend to a depth of 200 m.[5]

The upper limit to ocean temperatures is the temperature at which the cooling flux balances the full tropical solar flux. This is near 303 K (30 C) and is dependent on the wind speed. The high absolute humidity at these temperatures produces very unstable conditions once condensation starts. This results in the formation of intense thunderstorms and very strong convection that can

4

raise the altitude of the tropopause to 18 km.[8,9] The detailed flux data sets needed to analyze tropical ocean surface energy transfer are quite sparse. One such data set is available for the Pacific Warm Pool from the TRITON buoy located on the equator at longitude 156° E.[2]

Figure 3 shows selected TRITON buoy data for location 156° E, 0° lat. (equator) in the Pacific warm pool. Hourly average data are shown for July 1 to 15, 2010. Figure 3a shows the air temperature and the ocean temperatures at 1.5 and 25 m depth (SST 1.5 and SST 25). Figure 3b shows the wind speed and the solar flux. Over the period shown, the average air temperature was 301.2 K (28.2 C), SST 1.5 was 301.8 K (28.8 C) and SST 25 was 301.6 K (28.6 C). Both the air and the SST 1.5 temperatures exhibit a diurnal variation. The maximum daily excursion was 1.5 K for the air temperature and 1 K for SST 1.5. The SST 1.5 data shows a strong dependence on the wind speed. The maximum increase in daily temperature of 1 K on day 10 occurred with the wind speed near 1 m s^{-1}. The minimum increase in temperature of 0.1 K occurred on day 14 when the wind speed was in the 6 to 7 m s^{-1} range. There was a gradual drift in SST 25, but there was no diurnal variation at these depths.

There was also a variable time or phase shift between the noon peak of the solar flux and the SST 1.5 diurnal peak. This is shown in Figure 4 for days 10 to 15. The phase shift in hours and the total daily solar flux in MJ m^{-2} are shown for each of the 5 days. The phase shift decreases as the wind speed increases. This increases the surface evaporation and there is more downward transport of cooing water from the surface. It is also important to note that 1 to 2 MJ m^{-2}.day^{-1} variations in the total daily solar flux have no observable effect on the SST 1.5 diurnal temperature changes. An Excel model of the data shown in Figure 3 was constructed using the thermal reservoir approach described in Part I, Eqns (1-5) and the solar attenuation from Fig 11 with a simple ocean thermal mixing algorithm. This is described in more detail in Clark.[5] The total daily solar flux, calculated daily cooling flux and the daily average wind speed are plotted in Figure 5. The strong influence of the wind speed on the cooling flux can clearly be seen. An increase in average wind speed of 1 m s^{-1} increases the latent heat flux by approximately 2 MJ m^{-2} day^{-1}.

The increase in downward surface LWIR flux from an increase of 100 ppm in atmospheric CO_2 concentration is approximately 0.15 MJ m^{-2}.day^{-1}. This can have no measurable effect on ocean temperatures. It is simply absorbed within the first 100 micron ocean layer and dissipated as a minute part of the total surface cooling flux. It is also important to note that the absorbed solar flux is decoupled from the wind speed driven cooling flux. There is no 'equilibrium average' at the ocean surface on any time scale. The amount of heat stored in the ocean thermal reservoir depends simply on the accumulated net flux balance, including ocean transport effects.
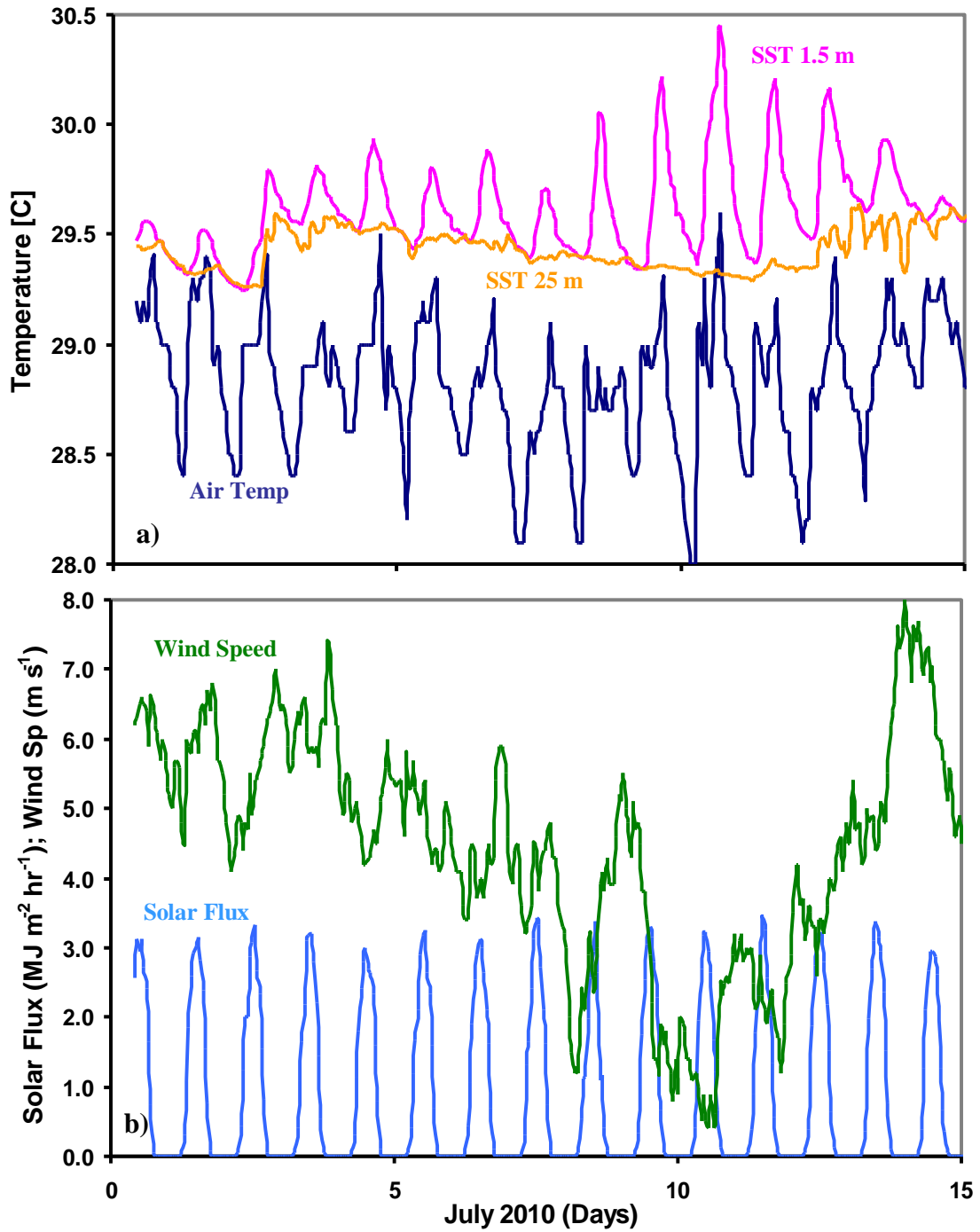
Figure 3: July 2010 TRITON buoy hourly data, 156° E, 0° lat., a) air and ocean temperatures (1.5 and 25 m), b) wind speed and solar flux.
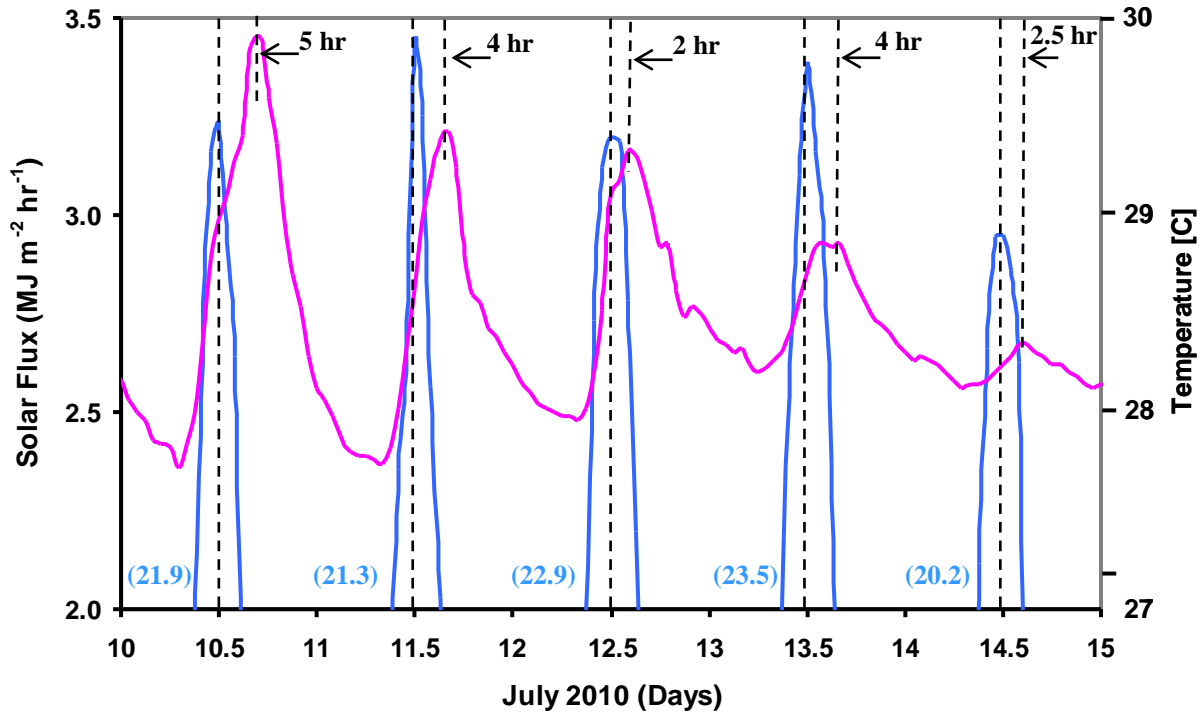
Figure 4: Phase shift between the 1.5 m ocean temperature and the solar flux, July 10 to 15, 2010. The values for the total daily solar flux (MJ m^{-2} day^{-1}) are also shown in parenthesis.
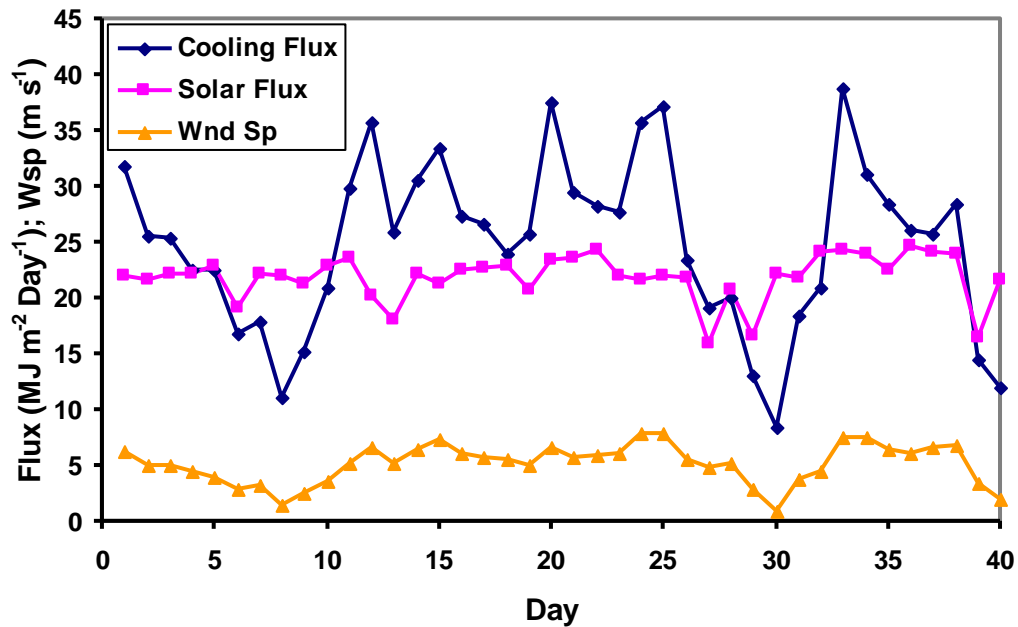

Figure 5: Total daily solar flux, modeled cooling flux and wind speed for the data shown in Figure 3. The strong influence of the wind speed can be clearly seen.

4. SURFACE ENERGY TRANSFER AT THE LAND–AIR INTERFACE:

Data sets containing sufficient information to analyze the flux balance at the Land-Air interface are quite sparse. Such data are available from a group of 7 monitoring sites in S. California operated by the University of Irvine as part of the Department of Energy Ameriflux Program. The 2008 data set recorded at the 'Grasslands' site, located in Limestone Canyon Regional Park, east of Irvine was analyzed in detail to investigate the surface energy transfer at the air-land interface.[3,5] The complete data set consisted of half hour averages of 17 parameters: friction velocity; air temperature; wind direction; wind speed; CO_2 flux; H_2O flux; sensible heat flux; latent heat flux; CO_2 concentration; H_2O concentration; incoming photosynthetic active radiation;, reflected photosynthetic active radiation; incoming global solar radiation; reflected global solar radiation; relative humidity; precipitation and net radiation.

Figure 6 shows the daily maximum and minimum measured air temperatures for 2008. The 8 day maximum and minimum surface (skin) temperatures from satellite data are also shown. The meteorological surface temperature (MSAT) is not the surface temperature, but the air temperature measured in an enclosure place at eye level, 1.5 to 2 m above the ground. The minimum air and surface temperatures are similar, but the maximum surface temperature during summer is approximately 15 K higher than the measured maximum air temperature because of convective mixing at the MSAT monitoring level. At this particular monitoring site, there were also well defined fluctuations in air temperature and humidity that were related to the shift from the ocean to the desert origin of the local weather system. Under ocean influences, temperatures were lower, the humidity was higher, and night and early morning clouds could develop. Under desert influences, the temperatures were higher and the humidity was lower. This site also experienced well known Santa Ana wind conditions when air that originates from the inland high desert regions is adiabatically compressed and produces very hot and dry conditions with very strong local winds. In order to examine the effect of solar heating and latent heat on the daily temperature rise, time series of the total daily surface heating flux (absorbed solar flux minus the daylight latent heat flux, MJ m^{-2} day^{-1}) and the daily temperature rise were plotted and scaled to overlap. This is shown in Figure 7. The total surface heating flux (thick line) shows the characteristic seasonal variation with a summer peak. Superimposed on this are decreases due to periods of cloud cover. The latent heat flux is derived from eddy covariance measurements that are not recorded during periods of rainfall. The daily temperature excursions generally follow the trend of the surface heating flux but with large fluctuations because of the transitions between ocean and desert influences.
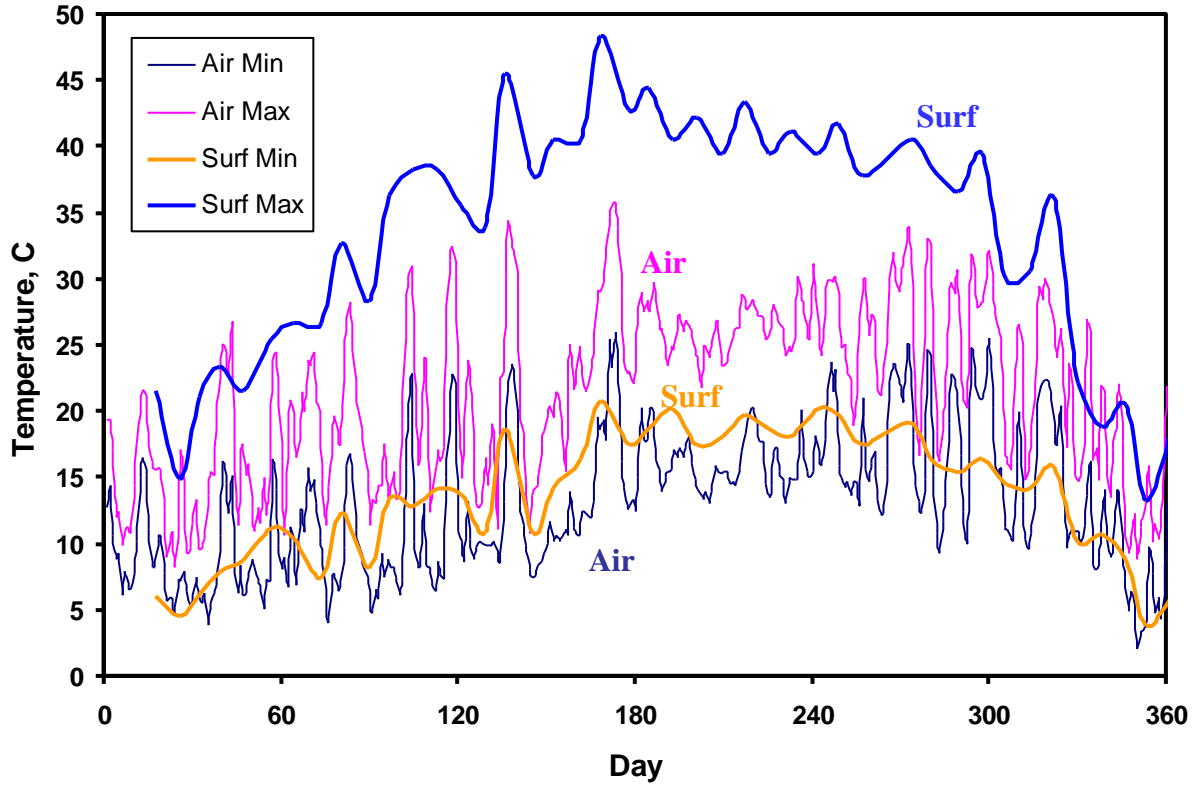
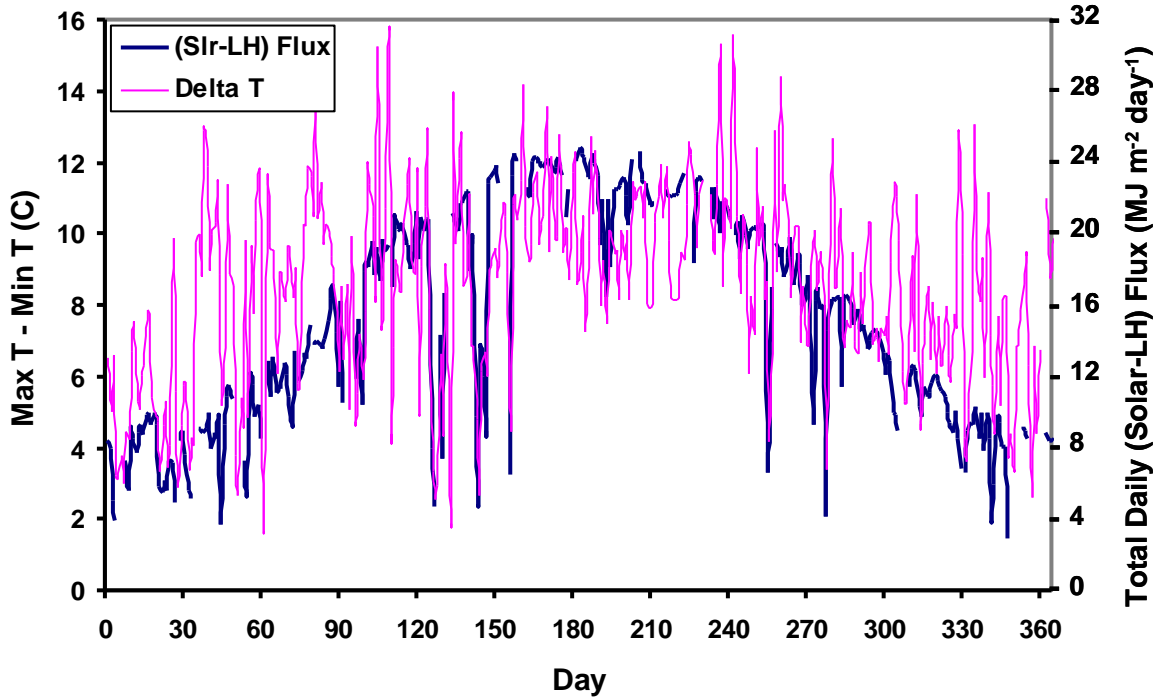**Figure 6: Maximum and minimum air and surface temperature data for 2008.**

Figure 7: Total daily (Solar-LH) flux (MJ m^{-2} day^{-1}) and daily temperature increase (Max-Min, K) for 2008

Figure 8 shows the daily total latent heat flux (MJ m^{-2} day^{-1}) for the daytime and night-time periods. Most of the flux is associated with the solar heating during the day. The seasonal peak in the latent heat flux occurs in the spring following the winter rainfall. It should also be noted that in the near IR (NIR) region, the solar flux can heat and evaporate water by direct NIR absorption in addition to the thermal heating of the land surface.
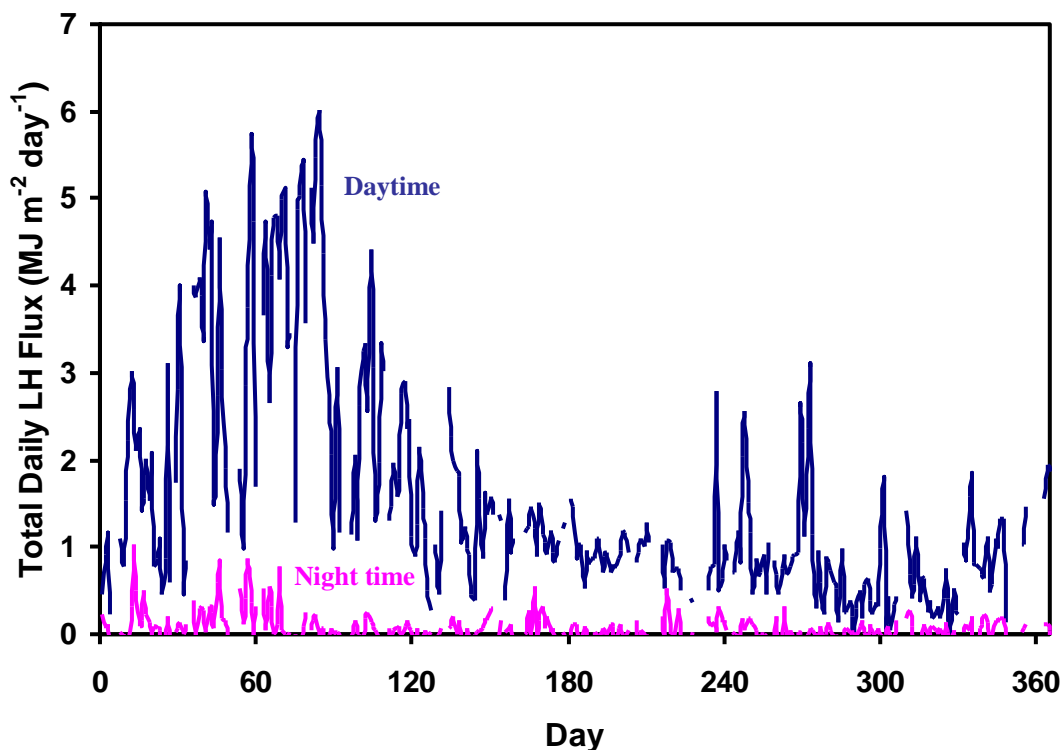

Figure 8: Daily latent heat flux totals (MJ m^{-2} day^{-1}) for daytime and night time evaporation

The effects of both humidity and cloud cover can be seen in the night time average IR flux. The average night time IR flux cooling flux was -43 ± 15 W m^{-2} (one sigma standard deviation). Under cloudy conditions, often associated with an early morning marine layer, the IR cooling flux was significantly reduced to values near zero. Under low humidity conditions, particularly those associated with fall Santa Ana winds, the IR cooling flux increased to nearly -100 W m^{-2}. The time series of the average night time IR flux is shown in Figure 9.
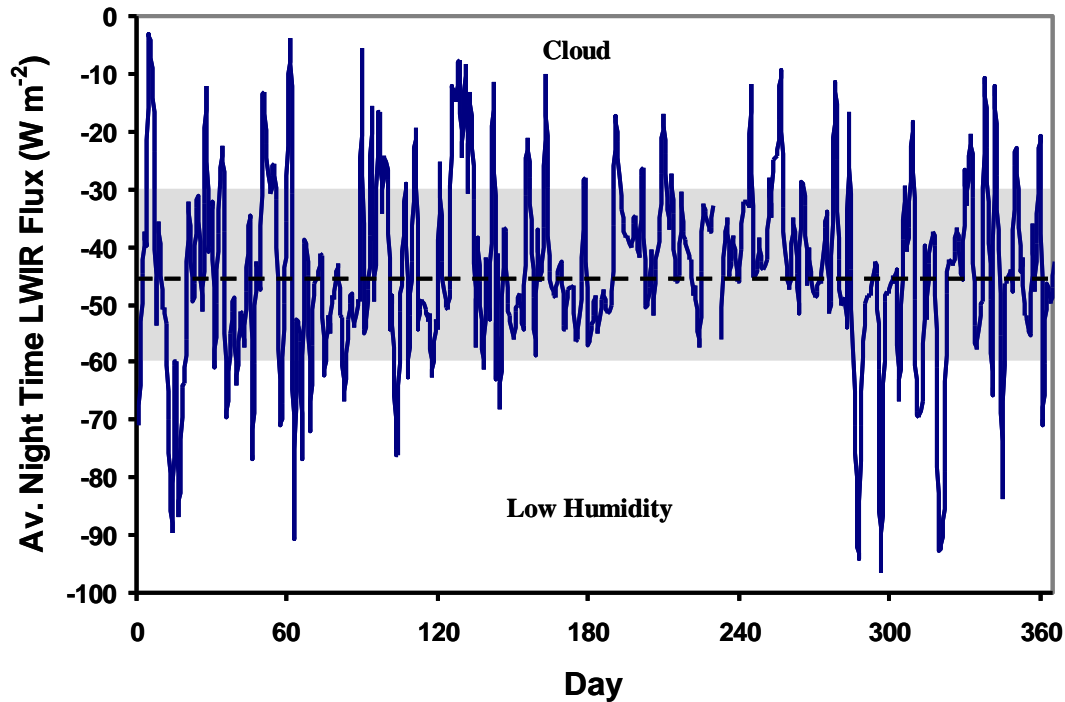
Figure 9: Time series of the average night time LWIR flux. The normal range of clear sky IR flux is approximately between -30 and -60 W m^{-2}. A LWIR flux between 0 and -30 W m^{-2} indicates low cloud cover. A LWIR flux <-60 W m^{-2} indicates low humidity conditions often associated with Santa Ana Wind conditions.

The coupled reservoir description given in Part I Eqns (1-7) was used to develop a simple Excel model of the surface energy transfer at the 'Grasslands' site. The energy balance of five flux terms, the absorbed solar flux, the net LWIR flux, the sensible heat, the latent heat and the subsurface conduction was used to calculate the temperature of the top 1 cm layer of the surface. Using this approach reasonable agreement between the calculated surface temperatures and the fit to the measured satellite surface temperatures is obtained. This is illustrated in Figure 10. Further details are given by Clark [5].
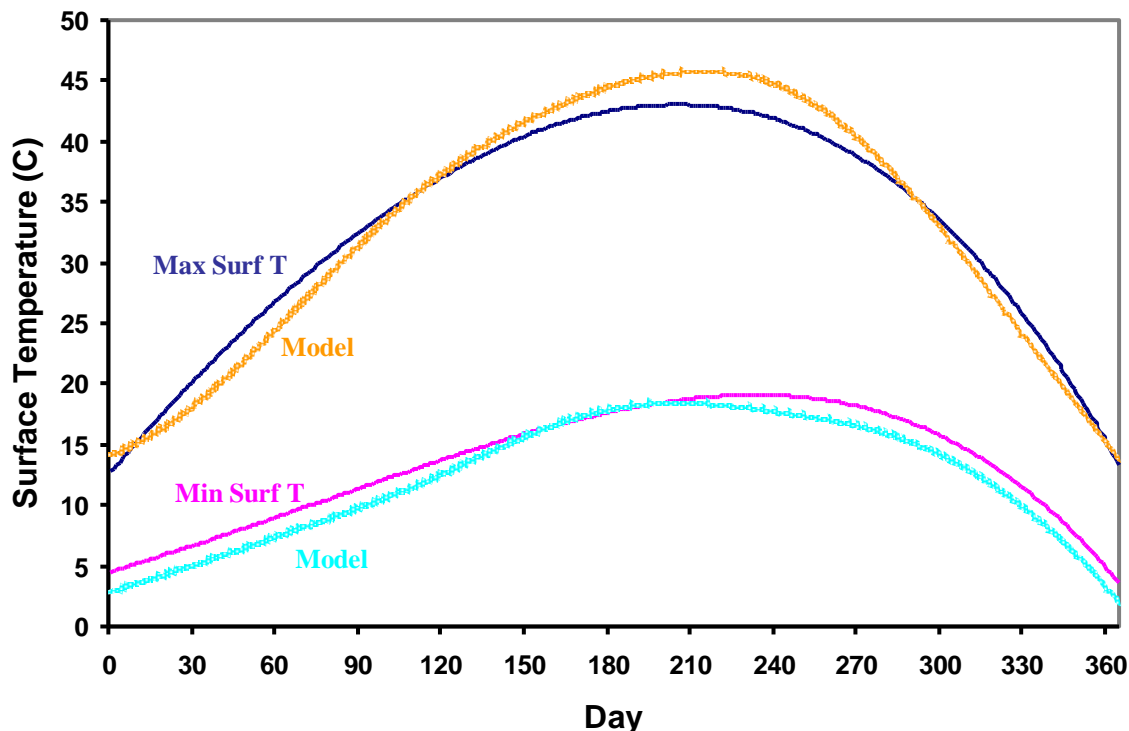
Figure 10: Calculated maximum and minimum temperatures compared to smoothed satellite surface temperature measurements derived from Figure 6.

The effect on the simulated surface temperatures of an increase of 1.7 W m^{-2} in the downward LWIR flux was investigated by decreasing the IR cooling term in the model from 43 to 41.3 W m^{-2}. This is the approximate increase in LWIR flux produced by a 100 ppm increase in the atmospheric CO^2 concentration. The average annual increases in the calculated minimum and maximum surface temperatures were 0.065 and 0.062 K. The daily differences are shown in Figure 11. All of the daily changes were between 0.060 and 0.067 K. The reason that these temperature changes are so small is because the change in LWIR flux is a small fraction of the daily heat flux dynamically coupled to the surface. A flux of 1.7 W m^{-2} corresponds to a daily cumulative flux of 0.15 MJ m^{-2}.day^{-1} that is superimposed on a total daily dynamic flux change in excess of 10 MJ m^{-2} day^{-1} coupled to a thermal reservoir with a heat capacity of 1.4 MJ m^{-3} K^{-1}. In practice, because of the daily fluctuations in the flux terms that were smoothed by the model averaging, the small changes shown in Figure 11 are not detectable in the surface temperature record. This result clearly demonstrates that any equilibrium assumption used to calculate the surface temperature is invalid. The change in heat flux must be coupled dynamically to the short term flux balance using a heat conduction model with realistic heat flux terms and surface thermal properties. A 100 ppm increase in atmospheric CO_2 concentration has no measurable effect on the surface temperature.
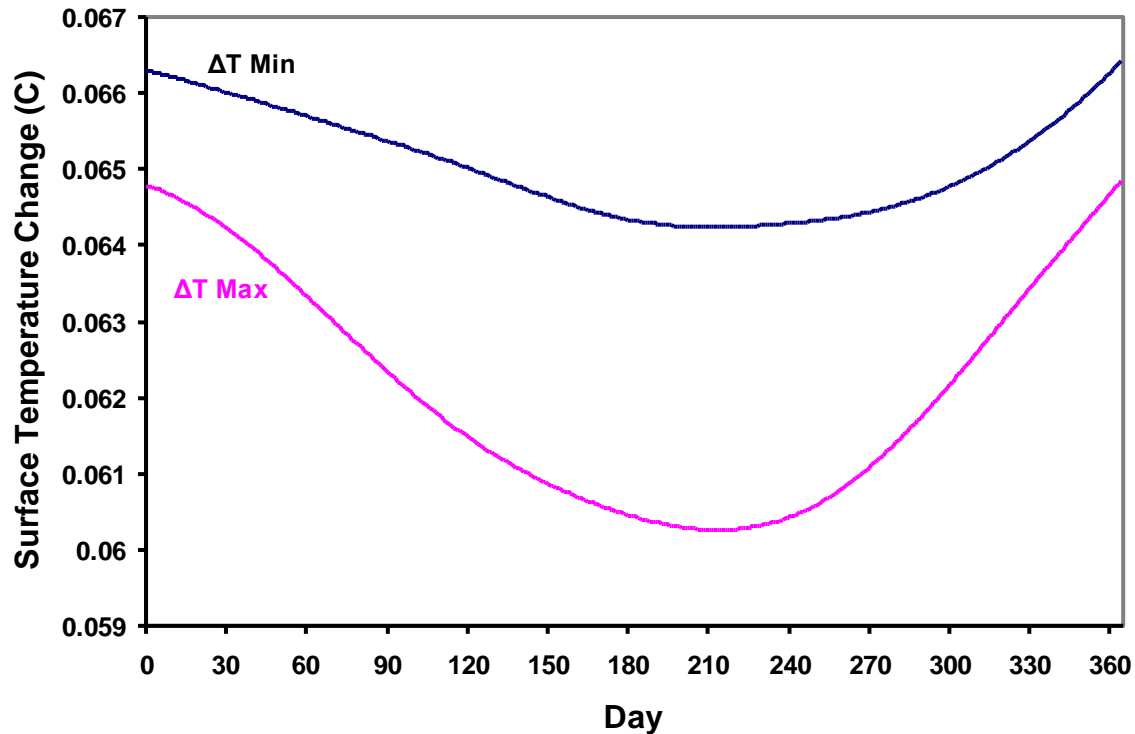
Figure 11: Effect of a 1.7 W m⁻² increase in downward LWIR flux on the calculated daily maximum and minimum temperatures.

Figure 12 shows the minimum surface and air temperatures for days 60 to 180 using the data from Figure 6. The daily minimum air temperature shows distinct spikes of approximately 10 K caused by the ocean-desert weather shift. The surface temperature clearly follows the air temperature, although the surface temperatures are 8 day satellite averages. The places where the satellite averaging closely follows the air temperature shifts are indicated by the arrows.[5]

Figure 12 illustrates the mechanism of the ocean influence on the seasonal and long term climate change in California and in other areas such as the UK as discussed in the next section. As the solar flux increases and the oceans warm in the spring and summer, the bulk air temperature of the prevailing weather systems increases. This in turn increases the evening transition temperature at which convection stops or is significantly reduced as given by Eqn (5) in Part I. More heat remains stored in the ground and the minimum MSAT temperature and surface temperatures increase. There is also a seasonal phase shift of approximately 6 weeks between the peak solar flux and the peak surface temperatures. Long term changes in ocean surface temperatures are also coupled into the bulk air temperatures of the weather systems and impact the convection transition temperature.
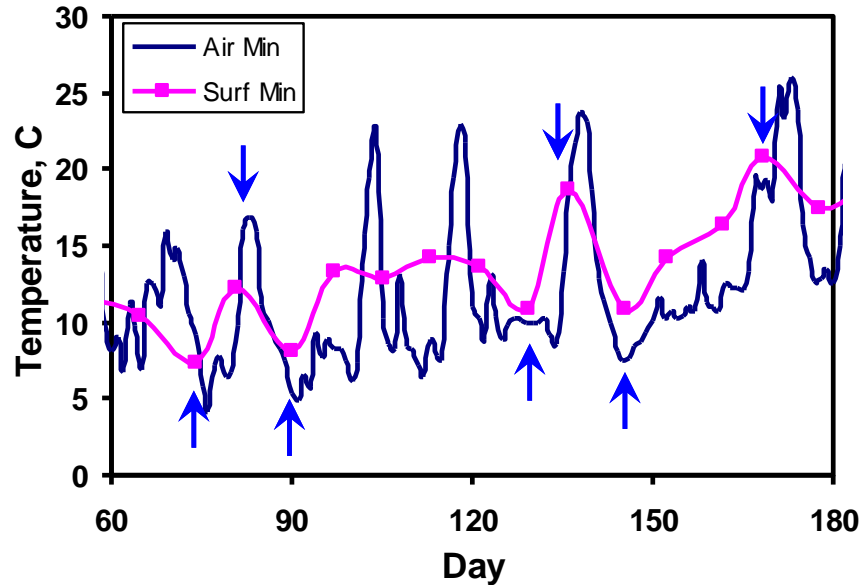
Figure 12: Minimum surface and air temperature for days 60 to 180 from Figure 6.

5. THERMAL STORAGE IN THE LOWER TROPOSPHERIC RESERVOIR

The nearest radiosonde recording station to the 'Grasslands' site is Miramar, San Diego, located approximately 100 km due south. Radiosonde data are recorded twice per day at midnight and noon UCT (Greenwich Mean Time).[4] This corresponds to local recording times in San Diego of 4 pm and 4 am Pacific Standard Time. At 4 pm, the surface convection peak has passed and the lower tropospheric reservoir is near its maximum average temperature. Conversely, at 4 am the lower tropospheric reservoir is near its minimum average temperature. Forty days of 2008 radiosonde data with 80 balloon ascents were analyzed. The ascents were selected to give four 10 day intervals centered on the solstice and equinox points. Temperatures from the lowest data recording level, 128 m and the first temperature recorded above the 2 km level were extracted from the radiosonde data. These are plotted separately for the 4 pm PST and 4 am PST ascents in Figure 13. At the surface (128 m level), the recorded night time temperatures were approximately 10 K lower than the daytime temperatures. At the 2 km level, for 30 out of 40 days, the day and night time 2 km level temperatures were similar to the night time surface temperatures. For the other 10 days, the 2 km levels were approximately 10 K lower than the night time surface levels. This variation was caused by the differences in weather systems at the monitoring site. Seven of the 10 days with lower night time temperatures were recorded in December.
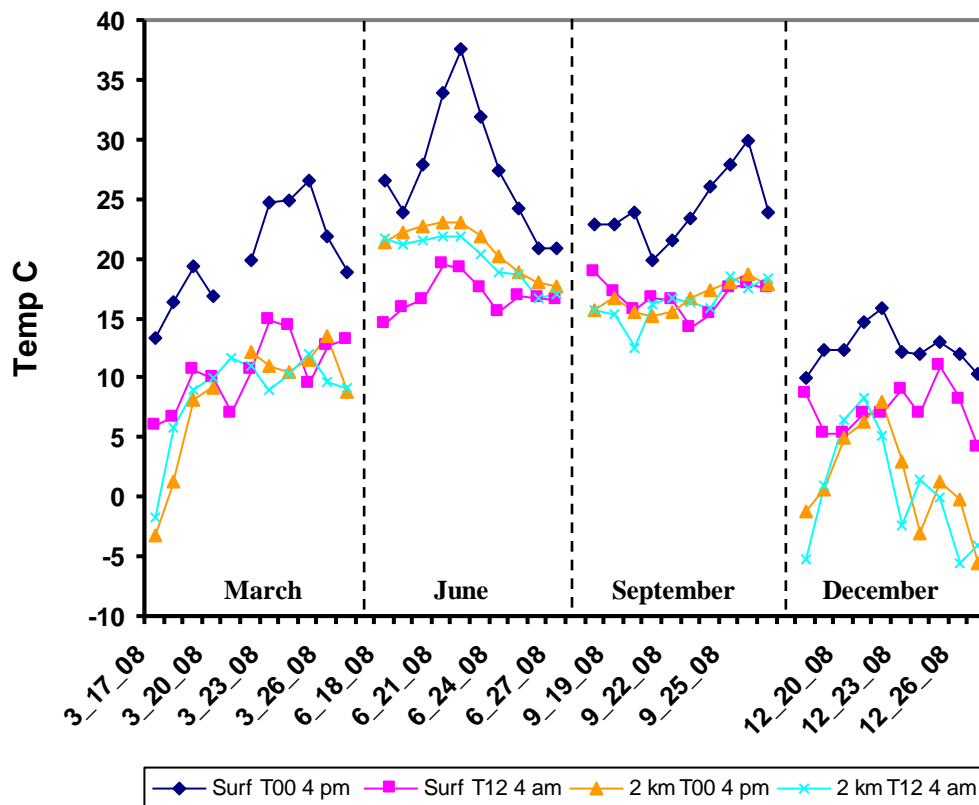
Figure 13: Measured surface (128 m) and 2 km temperature levels from San Diego (Miramar) 2008 radiosonde data. The daytime (4 pm PST) and night time (4 am PST) ascents are plotted separately. Ten day intervals at the equinox and solstice points are shown.

The average day and night time temperatures for the fully mixed 2 km air column were also calculated from the ascent data. These are shown in Figure 14. The difference in average column temperature between the day and night time datasets was only 1.6 ±1.6 K (one sigma standard deviation). The San Diego radiosonde data clearly illustrate the night time thermal storage properties of the lower tropospheric reservoir. However, they cannot be compared directly to the 'Grasslands' data because of the 100 km separation between the two monitoring sites.

The heat capacity of a 2 km x 1 m^2 air column in the lower troposphere is approximately 2 MJ K^{-1}. The 2 K temperature difference corresponds to a diurnal heat flux cycle of 4 MJ m^{-2} day^{-1}. An increase of 1.5 W m^{-2} in the LWIR flux from a 100 ppm increase in atmospheric CO_2 concentration is only 0.13 MJ m^{-2} day^{-1}. Fully coupled into the lower tropospheric reservoir, this would only produce a temperature rise of 0.07 K. Even this is too small to be measured in the day to day fluctuations of the reservoir temperatures.
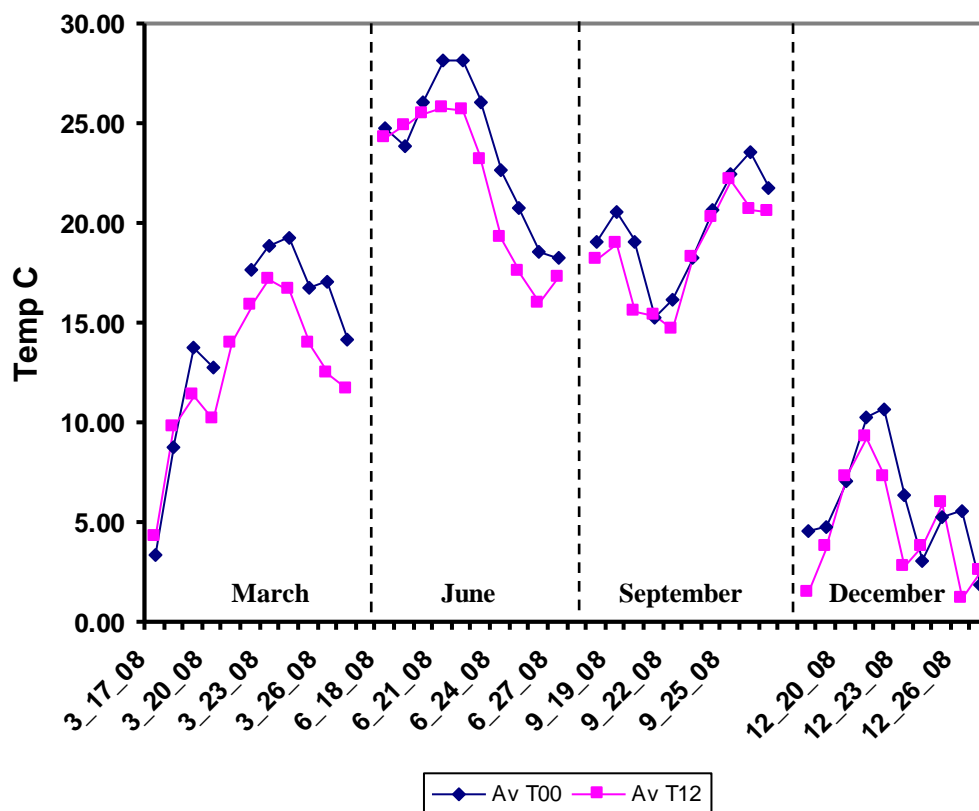
Figure 14: Average day and night time temperatures for the fully mixed 2 km air column calculated from Figure 13

6. THE INFLUENCE OF OCEAN TEMPERATURES ON THE METEOROLOGICAL RECORD

In many regions of the world, the observed changes in the MSAT climate record can be explained as a combination of changes in ocean surface temperatures, urban heat island effects and the 'adjustment' or 'homogenization' of the climate record.[5,6,10,11]   Changes in ocean temperatures are the dominant cause of the observed climate variations. The effects of both the PDO and the AMO can clearly be seen in the continental US temperature record. Ocean temperature effects may be studied by comparing the minimum MSAT record of a selected weather station to the appropriate ocean surface temperature record over the same period of record. For the State of California, and neighboring regions, the appropriate reference is the Pacific Decadal Oscillation, PDO and for the UK and surrounding regions, the appropriate reference is the local Atlantic Multi-decadal Oscillation, AMO.[12-15] Figure 15 shows the minimum MSAT for Los Angeles Civic Center, five year rolling average from 1925 to 2005. The PDO is also shown over the same period of record with the same 5 year averaging applied. The linear trend lines for both data sets from 1925 to 2005 are also shown. The minimum

MSAT data for the LA Civic Center shows the characteristic 'signature' of the PDO superimposed on an upward sloping baseline. The difference in slope between the PDO and the weather station data, 0.022 C yr^{-1} is an approximate indicator of the urban heat island effect for Los Angeles.
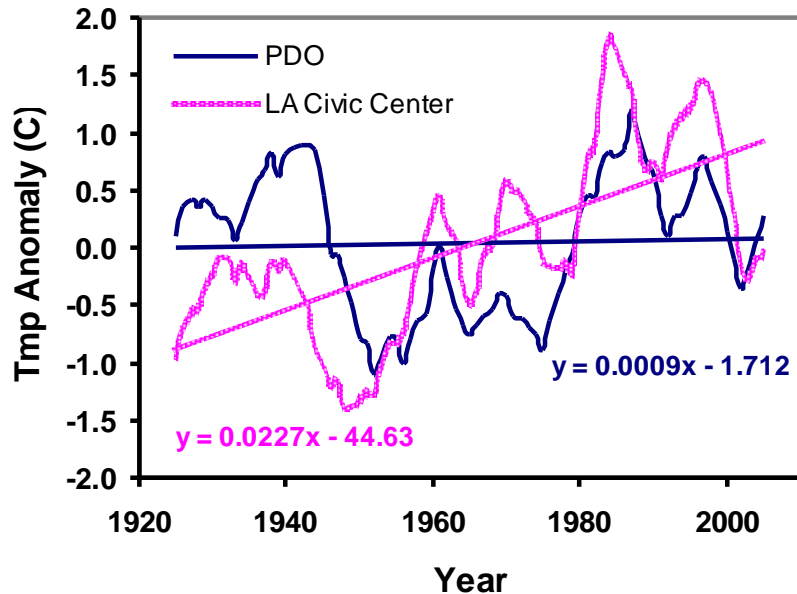

Figure 15: Minimum MSAT temperature, 5 year rolling average, for the LA Civic Center from 1925 to 2005. The PDO and the trend lines over the same time period are also shown.

Figure 16 shows the minimum MSAT for Los Angeles Airport, LAX, from 1950 to 2008 with the PDO and trend lines over the same period of record. In this case, the slope of the station data is close to that of the PDO. The slope difference is 0.005 C yr^{-1}. LAX is located on the coast, approximately 25 km west of the Civic Center. The marine layer and onshore flow at LAX significantly reduce the urban heat island effect compared to the Los Angeles Civic Center. The minimum MSAT trend data for LA Civic Center and LAX are examples of a general technique that compares the minimum MSAT data to a reference set of ocean surface temperatures along the approach path of the prevailing weather systems. While care is needed in the interpretation of such data, the difference in slope between the ocean reference and the station data is an approximate measure of the local urban heat island effect on the station. In addition, obvious discrepancies such as steps or unexpected peaks in the station data can be used to flag data anomalies for further investigation. Using this technique, a total of 34 California weather stations were analyzed. Stations with a minimum record duration of 50 years were selected to be representative of the full geographical and climate extent of California. The stations were divided into four groups, coastal, rural, urban and anomalous based on location and the magnitude of the slope difference. The linear trend data are plotted in Figure 17. Further details are given in Clark.[6]
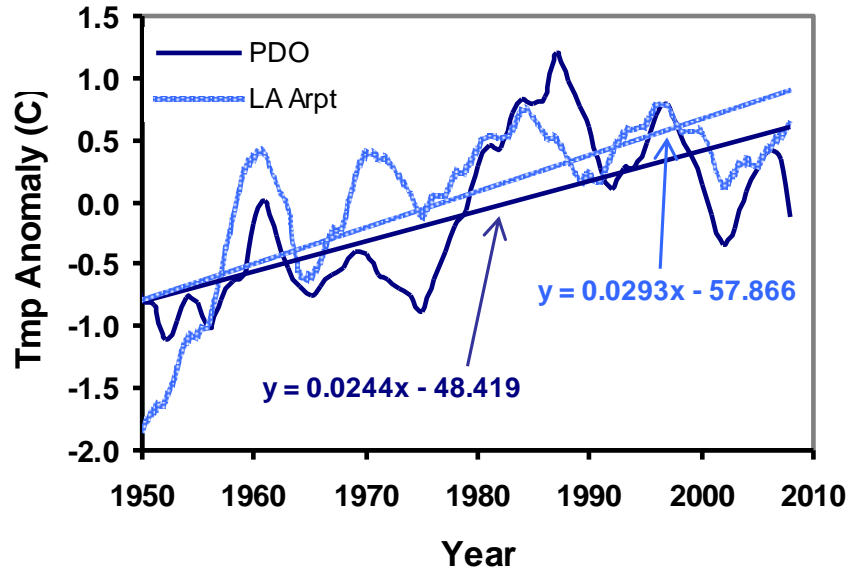
Figure 16: Minimum MSAT temperature, 5 year rolling average, for LA Airport from 1950 to 2008. The PDO and the trend lines over the same period of record are also shown.
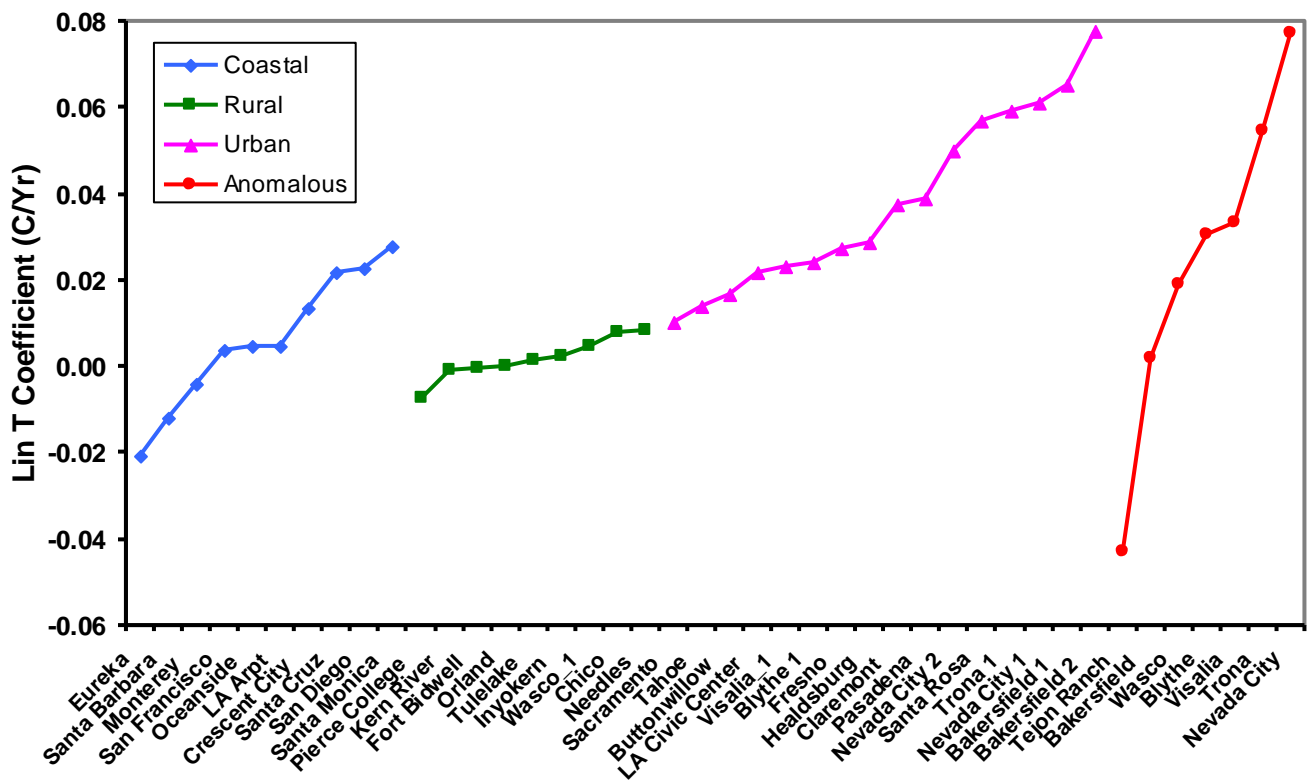

Figure 17: Linear warming trend data for the California weather stations. The stations were divided into four groups based on location and linear trend magnitude.

These results show that the climate of the State of California, as measured by the minimum MSAT weather station record is set mainly by the PDO. Superimposed on the PDO is an approximately linear urban heat island effect that depends on the local microclimate of the individual station and the influence of urban development on diurnal and seasonal subsurface heat storage. There is no evidence of a CO_2 induced global warming trend in the California data. Each station has its own unique microclimate and local bias effects. There is no common 'hockey stick' trend that can be correlated to CO_2.

The analysis of the minimum MSAT record for the 34 California weather stations was extended to 33 UK weather stations using the local Atlantic Multi-decadal Oscillation as the ocean surface temperature reference. Figure 18 shows the linear trend analysis for Heathrow, which had the largest urban heat island effect in the UK station data. Figure 19 shows the linear trend data for the 33 stations. These were divided into three groups based on the magnitude of the linear trend. There is no 'hockey stick' evidence of CO_2 induced global warming in the UK data.[5]
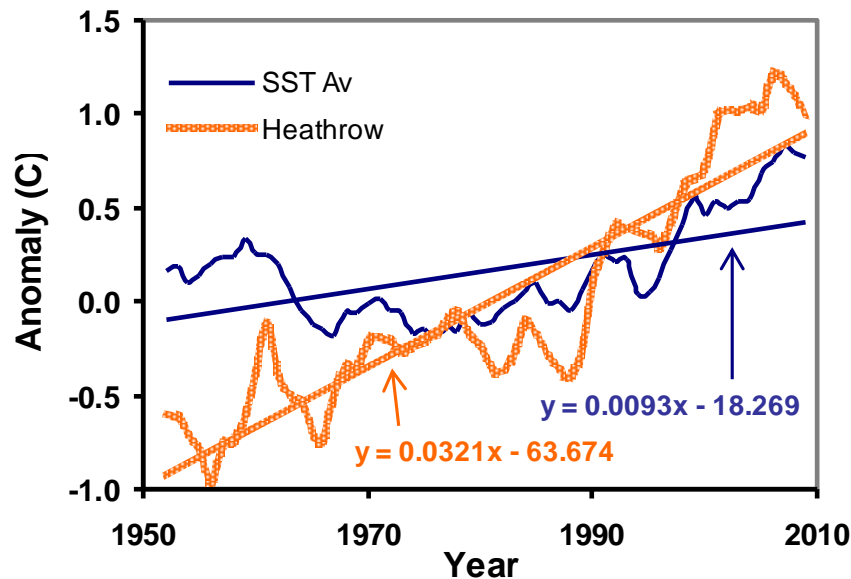

Figure 18: Linear trend analysis for Heathrow using the AMO as reference over the same period of record.

Overall, the linear trends for the UK stations showed lower urban heat island effects compared to the California stations. The UK linear trend range was from approximately -0.005 to +0.025 C yr^{-1}. The California linear trend range was from approximately -0.02 to +0.08 C yr^{-1} (excluding the anomalous station data). The urban heat island effect is a measure of the increase in heat stored in the ground (and structures) as a result of urban development. It depends on both the

solar heating of the area and the changes in latent heat flux as a result of urban run-off and vegetation loss. Since the UK receives less sunshine and more rainfall than most of California, the urban heat island effects are lower for the UK. The general climate trend for the UK is decreasing rainfall and increasing sunshine from N to S and W to E. This is reflected in the urban heat island trends. The higher trend values tend to be located in the SE. However, each station has its own microclimate that needs to be evaluated on a case by case basis. The 'one size fits all' practice of 'homogenizing' and averaging station data into 5° latitude and longitude 'boxes' overestimates climate change by adding urban heat island effects to the natural climate trends.[11]
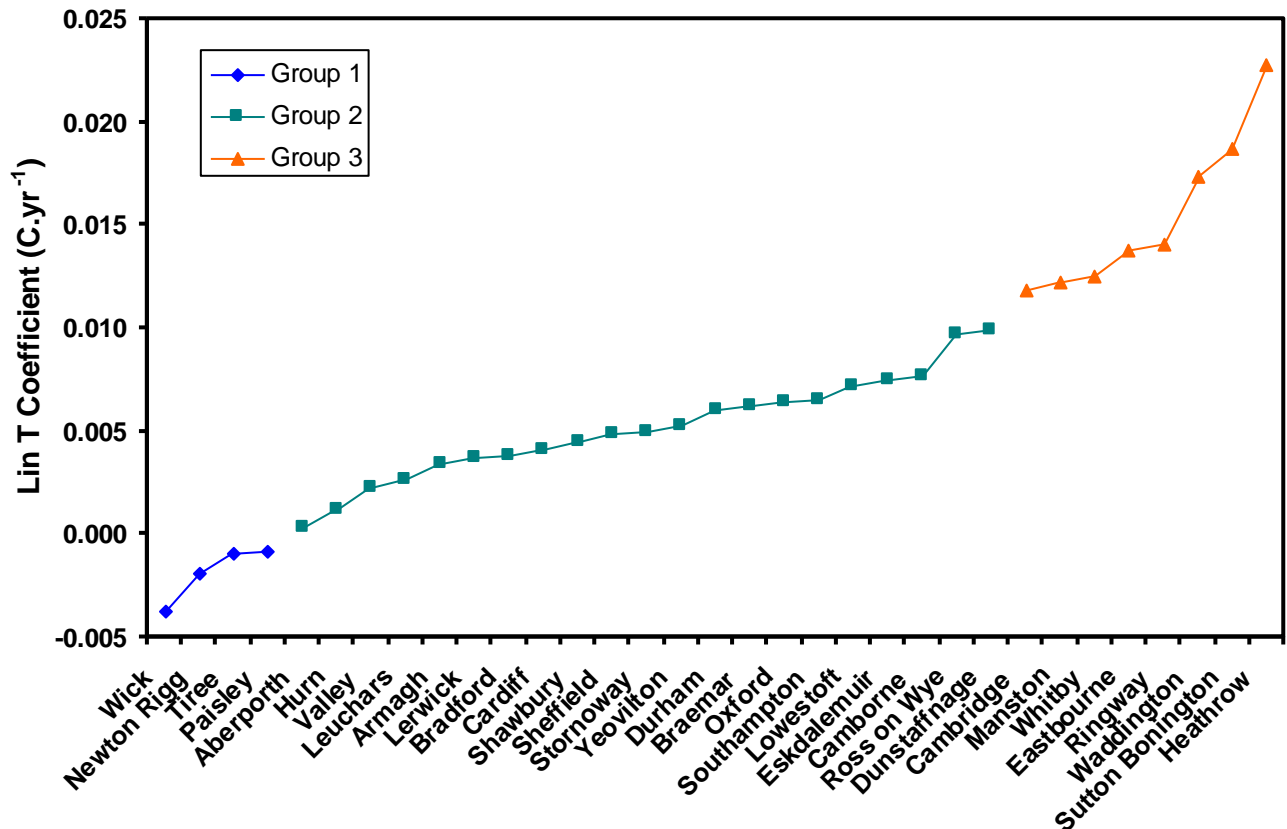

Figure 19: Linear warming trend data for the UK weather stations. The stations were divided into three groups based on linear trend magnitude.

7. CONCLUSIONS

The coupled thermal reservoir approach described in Part I has been demonstrated by analyzing flux and meteorological data covering a range of thermal reservoir conditions. These include ocean thermal storage at mid latitudes, the surface flux balance of the Pacific warm pool, the land surface flux balance at a S. California monitoring station and heating of the lower thermal

reservoir over San Diego, CA. In addition, long term climate trends in minimum MSAT data have been shown to follow the ocean surface temperatures in the region of formation of the prevailing weather systems. This was demonstrated using the PDO for California and the AMO for the UK. This approach also allows urban heat island effects and other weather station biases to be evaluated.

The effect of a 100 ppm increase in the atmospheric concentration of CO_2 on the measured data sets was also considered. The 100 ppm increase in concentration has produced an increase of approximately 1.5 W m^{-2} in the downward atmospheric LWIR flux reaching the surface. When this small increase in downward LWIR flux is added to the time dependent flux balance and coupled to the thermal reservoirs, it can produce no measurable increase in surface temperature. The magnitude of the individual heating and cooling flux terms, their large short term variations and the large heat capacity of the thermal reservoirs mean that any temperature change produced by the CO_2 flux is too small to measure. For example, the estimated increase in the surface temperature from the CO_2 flux for the 'Grasslands' land reservoir site in S. California was less than 0.07 K. This estimate was obtained using smoothed parametric fits to the flux data. When the flux variations in the original data are considered, a 0.07 K temperature increase is too small to be measured.

The data sets used in this analysis have only become available in recent years because of improvements in monitoring instrumentation and computerized data acquisition systems. There is a clear need to deploy much larger networks of such advanced monitoring instrumentation for both ocean and land measurement sites. The basic requirement for any climate model is that the results should explain the measured data. This should include the detailed dynamic flux balance at the measurement sites and the related phase shifts between the flux and temperature profiles. For the land thermal reservoir, such phase shifts were clearly identified by Fourier in 1827.[16] A priori assumptions about the role of carbon dioxide in climate change need to be replaced by validated engineering analysis of the dynamically coupled thermal reservoirs that form the Earth's climate system.

8. ACKNOWLEDGEMENTS

REFERENCES

1. Argo Profiling CTD Floats, 2012, NOAA Pacific Marine Environmental Laboratory, http://floats.pmel.noaa.gov/index.html

2. TRITON Data, 2012, http://www.pmel.noaa.gov/tao/jsdisplay/

3. Goulden, M. L., 2012, Ameriflux Data, Grasslands Site Data
   http://ameriflux.ornl.gov/fullsiteinfo.php?sid=193

4. U. Wyoming, sounding data, 2012, http://weather.uwyo.edu/upperair/sounding.html

5. Clark, R., The dynamic greenhouse effect and the climate averaging paradox, Ventura Photonics Monograph, VPM 001, Thousand Oaks, CA, 2011, Amazon.

6. Clark, R., CA Climate Change is Caused by the Pacific Decadal Oscillation, Not by Carbon Dioxide, SPPI Sept 16 th, 2010, http://scienceandpublicpolicy.org/originals/pacific_decadal.html

7. Clark, R., 'A null hypothesis for CO_2', 2010 Energy and Environment, **21**(4) 171-200.

8. Eschenbach, W., The thunderstorm thermostat hypothesis, Energy and Environment, 2010, **21**(4) 201-200.

9. Lindzen, R. S., Chou, M.D. and Hou, A.Y., Does the Earth have an adaptive IR iris? Bull Amer Met Soc 2001, **82**(3) 417-432.

10. D'Aleo, J., 'Effects of AMO and PDO on temperatures', Intellicast, May 2008.   , http://www.intellicast.com/Community/Content.aspx?a=127

11. D'Aleo, J. '*Progressive Enhancement of Global Temperature Trends*', Science and Public Policy Institute, July 2010. http://scienceandpublicpolicy.org/originals/progressive_enhancement.html

12. PDO Data, 2012, http://jisao.washington.edu/pdo/PDO.latest

13. HadSST2 Sea Surface Temperature Database, 2012, http://www.cru.uea.ac.uk/cru/data/temperature/,.

14. Western Region Climate Data, 2012, http://www.wrcc.dri.edu/Climsum.html,

15. UK Historical Climate Data, 2012, http://www.metoffice.gov.uk/climate/uk/stationdata/,

16. Fourier, B.J.B., Memoire sur les temperatures du globe terrestre et des espaces planetaires Mem. R. Sci. Inst. 1827, **7** 527-604